Article

Synthesis and Characterization of Stabilized Subnanometric Cobalt Metal Particles

Eva Barea, Xavier Batlle, Patrick Bourges, Avelino Corma, Vicente Forns, Amlcar Labarta, and Vctor F. Puntes

J. Am. Chem. Soc., **2005**, 127 (51), 18026-18030• DOI: 10.1021/ja053746b • Publication Date (Web): 06 December 2005

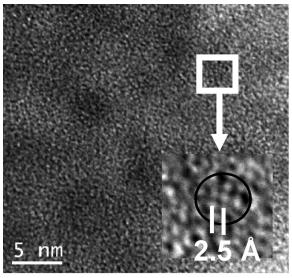

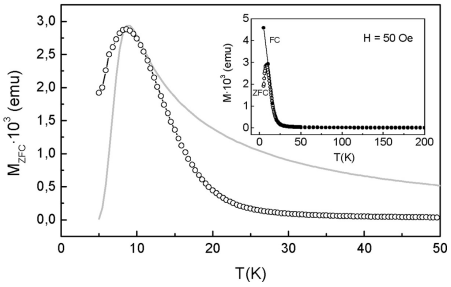

More About This Article

Additional resources and features associated with this article are available within the HTML version:

- Supporting Information
- Links to the 1 articles that cite this article, as of the time of this article download
- Access to high resolution figures
- Links to articles and content related to this article
- Copyright permission to reproduce figures and/or text from this article

View the Full Text HTML

J|A|C|S
ARTICLES
Published on Web 12/06/2005

Synthesis and Characterization of Stabilized Subnanometric Cobalt Metal Particles

Eva Barea,[†] Xavier Batlle,[‡] Patrick Bourges,[||] Avelino Corma,*[,†] Vicente Fornés,[†] Amílcar Labarta,[‡] and Víctor F. Puntes*[,‡,§]

Instituto de Tecnología Química, UPV-CSIC, Av. los Naranjos s/n, Valencia, Departament de Física Fonamental, Universitat de Barcelona, 647 Av Diagonal, 08028 Barcelona, Spain and Institut Français du Pétrole 1−4 avenue de Bois-Préau 92852 Rueil-Malmaison Cedex, France

Received June 8, 2005; E-mail: acorma@itq.upv.es; Victor.Puntes@uab.es

Abstract: Subnanometric cobalt metallic particles, with an average size of 0.8 nm and an estimated number of 50 atoms, have been stabilized in the confined spaces within the nanopores of crystalline molecular sieves. Remarkably, these clusters show a rapid vanishing of the magnetization as the temperature is increased from 10 to 20 K because of the ferromagnetic−paramagnetic transition together with thermal fluctuations of the remaining moment. This dramatic reduction of the transition temperature is due to strong finite size effects. Such behavior, predicted for very small metallic particles, was never observed before due to the inherent difficulty in achieving subnanometric stable metallic particles.

Introduction

It is commonly expected, and often observed, that the structure and properties of nanostructured materials differ from those of the bulk. Thus, the ability to manufacture and control the structure of nanoparticles allows the design of materials with desired properties, and progression in understanding the genesis of the solid state.[1] Special attention is deserved by clusters of a reduced number of atoms, where a molecular regime is approached. For example, several measurements on 3d metal clusters evidence an enhanced magnetic moment per atom,[2,3] or the appearance of ferromagnetism in 4d metals.[4] One of the most explored cases is Au, where, for example, an extreme size sensitivity of catalytic activity is observed when the cluster size is reduced below 1 nm,[5] or surfactant-induced ferromagnetism appears.[6] Such findings have been somehow limited to Au due to its chemical stability, since clusters of other metals such as cobalt are extremely reactive, and their study outside the production device poses serious problems.

In this work we prepared open-air stable subnanometric cobalt metal particles to study magnetism in extremely small ferromagnetic particles. Cobalt was chosen because of its wide technological applications and rich nanometric behavior.[7,8] Regarding ferromagnetic materials, the magnetic moment and its temperature dependence are perhaps the most significant properties.[2] The ferromagnetic−paramagnetic transition temperature, known as the Curie temperature in a ferromagnet, T_c, gives an idea of the amount of energy that it takes to break up the long-range ordering in the system (T_c for bulk cobalt is 1388 K). T_c depends on the strength of the atomic magnetic coupling, and it is strongly affected by finite size effects.[9] Investigations on T_c for single cobalt layers are highly dependent on structural details, and a broad range of results, around 100 K, have been reported.[10]

To stabilize cobalt clusters, we have applied a synthetic strategy that involves the synthesis of zeolite structures in which cobalt atoms are substituting for silicon at framework positions. Silica and cobalt were supplied by a previously synthesized crystalline layered cobalt silicate with magadiite structure.[11] Thus, by coupling the rate of dissolution of the layered compound and the nucleation rate of the zeolite, BetaCo and ZSM-5Co zeolites have been synthesized, in which cobalt is not ion exchanged but occupies framework positions. Mild heat treatments—calcination—performed to remove the organic structure-directing agents (tetraethyl—and tetrapropyl—ammonium) make the sample transpire a small amount of cobalt, under a reducing atmosphere,[12] which locates within the cavities of the zeolite. The cavity limits the growth of the cobalt clusters and passivates them against oxidation, even if the pore diameter of the zeolites is big enough for oxygen to pass through.

[†] UPV-CSIC.
[‡] Universitat de Barcelona.
[||] Institut Français du Petrole.
[§] Current address: Insitut Català de Nanotecnologia, Campus UAB, 08163 Bellaterra, Spain.

(1) Alivisatos, A. P.; et al. *Adv. Mater.* **1998**, *10*, 1297.
(2) Billas, I. M.; Chatelain, A.; de Heer, W. *Science* **1994**, *265*, 1682.
(3) Respaud, M.; et al. *Phys. Rev. B* **1998**, *57*, 2925.
(4) Cos, A. J.; Louberdack, J. G.; Apsel, S. E.; Bloomfield, L. A. *Phys. Rev. B* **1994**, *49*, 12295.
(5) (a) Haruta, M.; Yamada, N.; Kobayashi, T.; Lijita, S. *J. Catal.* **1989**, *115*, 301. (b) Carrettin, S.; Concepción, P.; Corma, A.; López-Nieto, J. M.; Puntes, V. F. *Angew. Chem., Int. Ed.* **2004**, *43*, 2538.
(6) Crespo, P.; et al. *Phys. Rev. Lett.* **2004**, *93*, 87204.
(7) Puntes, V. F.; Krishnan, K.; Alivisatos, A. P. *Science* **2001**, *291*, 2115.
(8) Skumryev, V.; Stoyanov, S.; Zhang, Y.; Hadjipanayis, G.; Givord, D.; Nogues, J. *Nature* **2003**, *423*, 850.
(9) Tang, Z. X.; Sorensen, C. M.; Klabunde, K. J.; Hadjipanayis, G. C. *Phys. Rev. Lett.* **1991**, *67*, 3602.
(10) Schneider, C. M.; Bressler, P.; Schuster, P.; Kischner, J. *Phys. Rev. Lett.* **1990**, *64*, 1059.
(11) Barea, E. M.; Fornés, V.; Corma, A.; Bourges, P.; Guillon, E.; Puntes, V. F. *Chem. Commun.* **2004**, *17*, 1974.
(12) Amiens, C.; de Caro, D.; Chaudret, B.; Bradley, J. S.; Mazel, R.; Roucau, C. *J. Am. Chem. Soc.* **1993**, *15*, 11638.

10.1021/ja053746b CCC: $30.25

Experimental Section

Synthesis. ZSM5Co and BetaCo zeolites were synthesized using as the source of silica and cobalt a Co-magadiite with a Si:Co atomic ratio of 50. This Co-magadiite was obtained by preparing a synthesis gel with the following molar ratio: SiO_2:0.2 NaOH:0.5 *trans*-4-aminocyclohexanol:15 H_2O:0.2 $Co(CH_3COO)_2$. After stirring, the gel was transferred to a Teflon-lined autoclave and heated at 423 K for 3 days. For Beta zeolite, 0.088 g of NaCl and 0.215 g of KCl were dissolved in a solution of 15.4 g of tetraethylammonium hydroxide in 8.58 g of water. A 4.402 g portion of Co-magadiite was added under stirring. Then, 0.275 g of sodium aluminate, 0.056 g of NaOH, and 2.92 g of water were added. In the case of ZSM5Co, a gel was prepared with 15.19 g of Co-magadiite, 151.19 g of water, 1.68 g of $Al_2(SO_4)_3 \cdot 18H_2O$, 1.519 g of NaOH, and 20.112 g of tetrapropylammonium bromide. The synthesis mixtures were loaded in Teflon-lined stainless steal autoclaves and heated at 448 and 413 K under rotation for 15 and 6 days, respectively. The solids obtained were washed with distilled water and dried at 373 K overnight. The heat treatment—calcination—which removes the organic agents and segregates the Co clusters studied in this paper, consists of 4 h at 540 °C (including the 3°/min heating ramp) under N_2 and 6 h more at 540 °C open to air.

Microscopy. The samples were examined by bright-field and dark-field transmission electron microscopy in a Hitachi 800MT microscope operated at an accelerating voltage of 200 kV and an HRES JEOL field emission microscope also working at 200 kV, employed for high-resolution and electron energy loss spectroscopy. Low-dose imaging was carried out to avoid zeolite damage. Dark-field experiments consist of observing the image produced by the diffracted electrons corresponding to a determined lattice spacing, leaving the rest dark. The samples were ground to a fine powder, diluted in ethanol to give a 1:3 volume ratio, and sonicated for 2 min. A Cu grid covered with a thin film of amorphous carbon was dipped in the methanol slurry and then allowed to dry covered by a watch. The contrast of the observed clusters is low since they are small and embedded in the matrix.

X-ray Photoelectron Spectroscopy (XPS). X-ray photoelectron spectra were acquired on a VG Escalab 210 spectrometer with an electrostatic hemispherical analyzer and a nonmonochromatized Al Kα X-ray source ($h\nu = 1486.6$ eV). The measurements were performed in the constant pass energy mode (50 eV). The X-ray gun was powered to 200 mW. The base pressure in the analysis chamber during spectrum acquisition was maintained at 4.0×10^{-9} mbar. The binding energies of the Co2p spectra were referenced to the C1s peak at 284.5 eV. The Auger parameter α′ of Co is defined as $\alpha' = E_b(Co2p_{3/2}) + E_k(CoL_{2,3}M_{4,5}M_{4,5})$.

Magnetometry. Magnetization measurements were performed in a SQUID magnetometer (MPMS 5S from Quantum Design) in a range between 1.8 and 300 K and up to 50 kOe. A 10 mg portion of the sample powder was normally measured. The experiments were repeated and the results reproduced.

X-ray Diffraction (XRD). Powder diffraction experiments were performed in an X'pert diffractometer using Cu Kα radiation, a graphite monochromator, and automatic divergence slits.

UV−Vis. Diffuse reflectance UV−vis spectra of pressed powders were recorded on a Cary 5G spectrophotometer using a Praying Mantis accessory and $BaSO_4$ as the reference.

Results and Discussion

XRD patterns of the synthesized and calcined cobalt-containing samples (see the Supporting Information (S1)) give the characteristic peaks of Beta and ZSM-5 zeolites, and no diffraction peaks of either magadiite or crystalline cobalt phases were detected. This is already a first indication that cobalt particles formed during the calcination process should be smaller than 2−3 nm.[11] The UV−vis spectra (see the Supporting Information (SI)) show, in addition to the Co−O electron-charge-transfer band at 200−210 nm, the characteristic triplet at 530, 590, and 640 nm corresponding to tetrahedrally coordinated cobalt.[13,14] This type of signal could be produced by cobalt in the framework or cobalt in exchange positions. To test the second hypothesis, CoBeta was repeatedly exchanged with NaCl. No cobalt was detected in the wash water, and the UV−vis spectrum of the "exchanged" solid remained unchanged. Thus, from the above results, we conclude that the metal cation is tetrahedrally coordinated, and we can assume that it is in the framework of the zeolite.

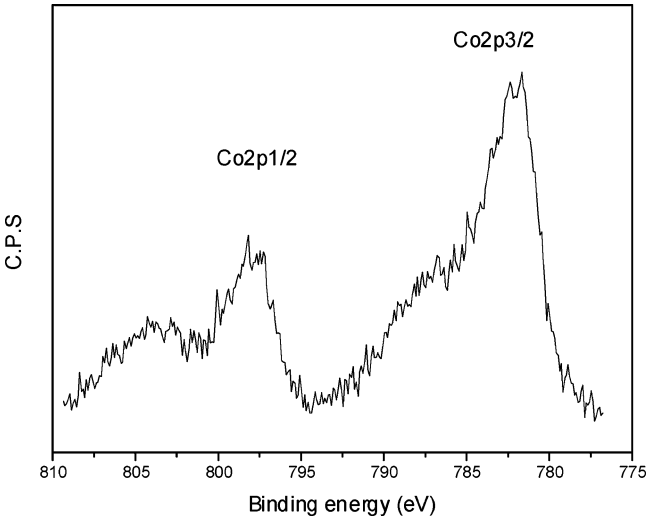

Figure 1. XPS spectra of the BetaCo sample. The energy gap between Co2p spin−orbit doublets is 16 eV, in agreement with the presence of high-spin Co^{2+} species. The position of the main line (782.1 eV) corresponds to highly disperse metallic atoms, typically framework atoms.

X-ray photoelectron spectra of the BetaCo zeolite show the binding energy of the $Co2p_{3/2}$ main line at 782.1 eV (Figure 1). At a 4.6 eV higher binding energy there is a satellite peak with an intensity ratio of the satellite to the main peak of 0.7, which is typical of high-spin Co^{2+} species.[15−17] The binding energy of the $Co2p_{3/2}$ peak (782.1 eV) cannot be ascribed to CoO (780.1 eV) or $Co(OH)_2$ (780.9 eV), but could be related to a combination of the Madelung potential and relaxation effects due to dispersed cobalt ions in an inorganic framework. It is well-known that Co^{2+} ion exchanged in Co-mordenite and $CoNH_4$-ferrierite zeolites show high binding energies (783−782.5 eV)[18] while cobalt ions in framework positions of CoAPO-11 and -36 are characterized by binding energies as high as 781.6 eV.[19] In our case no cobalt in exchange positions has been detected; consequently, we can again conclude that cobalt ions are dispersed in the framework of Beta zeolite. On the other hand, the Auger parameter of cobalt in the BetaCo sample (1552 eV) is different from that observed for CoO and $Co(OH)_2$ compounds (1550 eV),[14,15] confirming the absence of CoO and/or $Co(OH)_2$ in our sample.

Low and moderate transmission electron microscopy (TEM) resolutions show prismatic and shapeless zeolite crystals of size

(13) Verberckmoes, A. A.; Weckhuysen, B. M.; Schoonheydt, R. A. *Microporous Mesoporous Mater.* **1998**, *22*, 165.
(14) Hartmann, M.; Kevan, L. *Res. Chem. Intermed.* **2002**, *28*, 625.
(15) Mathew, T.; Shiji, N. R.; Sreekumar, K.; Rao, B. S.; Copinath, C. S. *J. Catal.* **2002**, *210*, 405.
(16) Dillard, J. G.; Koppelman, M. H. *J. Colloid Interface Sci.* **1982**, *87*, 46.
(17) Frost, D. C.; McDowell, C. A.; Woosly, I. S. *Mol. Phys.* **1974**, *27*, 1473.
(18) Jirka, I. *J. Phys. Chem. B* **2001**, *105*, 1140.
(19) Chao, K. J.; Wei, A. C.; Wu, H. C.; Lee, J. F. *Catal. Today* **1999**, *49*, 277.

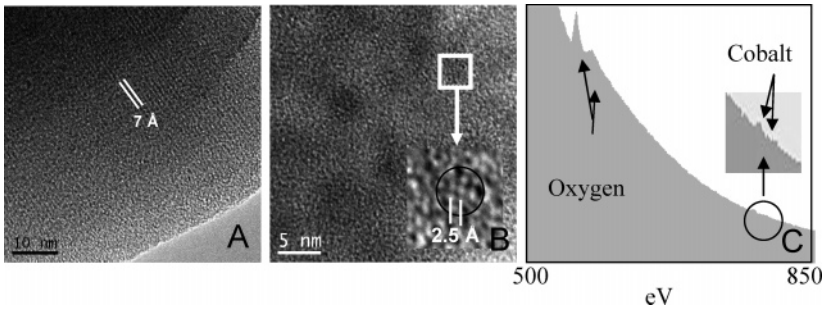

Figure 2. HRTEM of the BetaCo samples: (A) regular structure of the zeolites showing a periodicity of 7 Å, corresponding to the larger space available, (B) cobalt cluster (the fact that clusters are small and embedded in a matrix considerably diminishes the contrast), (C) EELS spectra of the same area where cobalt (metallic or not) is detected and the oxygen is mainly coming from the matrix.

within ~30 to 300 nm (Supporting Information (S2)). No high-electron-density spots are observed, and there is no diffracted contrast in the dark-field images, indicating the absence of metallic particles within the microscope resolution, which is in agreement with the XRD results. However, high-resolution TEM working up to a 1 million magnification shows clusters (0.8 nm in diameter) of atoms which appear slightly larger than the rest, with an interatomic distance around 0.25 nm that corresponds to the hcp metallic cobalt (the Co^{2+} radius is 0.08 nm, that of O^{2-} is 0.14 nm, and the CoO distance is 0.21 nm).[20] Electron energy loss spectroscopy (EELS) analysis of the same area (with a 10 nm spot around the observed cluster) indicates the presence of a small amount of metal cobalt (Figure 2).

Summarizing, structural characterization of calcined samples is consistent with the presence of Co^{2+} in the zeolitic framework, the absence of either CoO or $Co(OH)_2$ particles, and the presence of very small amounts of metallic cobalt.

The magnetic behavior of these samples showed an extremely low value of the temperature at which the ferromagnetic−paramagnetic transition in the metallic cobalt clusters takes place. This transition simultaneously competes with the thermal fluctuations of the magnetic moment of the clusters. Thus, when the samples are cooled in the absence of a magnetic field (zero-field cooling, ZFC), a random distribution of cluster magnetizations freezes, the total magnetization of the system being zero. If now the magnetization is measured by increasing the temperature and applying simultaneously a small magnetic field (50 Oe), the magnetization first increases as the cluster moments are progressively unblocked and able to align toward the applied field (Figure 3). After reaching a maximum (blocking temperature $T_B = 9$ K), the magnetization decreases due to thermal agitation of the magnetic moment (superparamagnetism, SPM), together with a decrease of the magnetic moment per particle itself. This gives rise to a very sharp peak in the ZFC curve. This peak is significantly narrower than that corresponding to a pure SPM relaxation process of monodisperse cobalt clusters of the same size and T_c over 100 K (see the gray line in Figure 3), or than that corresponding to cobalt clusters of about 150 atoms as reported in ref 3. Besides, when the sample is cooled in the presence of a small magnetic field (field cooling, FC), the cluster magnetizations become progressively blocked, favoring the direction of the applied field, and a remanence is found, which increases monotonically as the temperature decreases, indicating the absence of any observable magnetic interaction

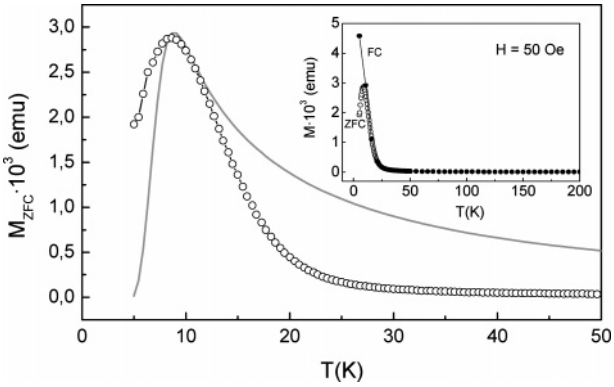

Figure 3. Magnetic susceptibility of BetaCo samples: ZFC curve measured at 50 Oe for the BetaCo sample. The gray line corresponds to the theoretical SPM relaxation of nearly monodisperse cobalt clusters 0.8 nm in size. Inset: ZFC and FC curves plotted at temperatures up to 200 K.

between clusters.[21] From the ZFC peak we can estimate an effective anisotropy of 8×10^6 J/m^3, which is significantly higher than the bulk one, likely due to surface effects and interactions of the cluster surface with the matrix, as previously observed.[23,23]

In the narrow temperature range between the mean blocking temperature and T_c, the assembly of metallic cobalt clusters behaves as a true SPM material with a decreasing magnetic moment, for which the magnetization curves as a function of the magnetic field, **M**(**H**), enable extraction of the magnetic moment per cluster, μ_c, and the width of the size distribution. This is done by fitting **M**(**H**) to a log-normal distribution of Langevin functions,[24] with a width of $\sigma = 0.47$. The fit perfectly follows the experimental data at all measured T values (Figure 4a). The fact that the magnetization relaxation is not simply SPM is clearly observed in Figure 4b, where the magnetization curves are plotted with the field divided by their corresponding measuring T. In SPM materials, these curves should collapse.[25]

The T dependence of the magnetic moment per cluster, $\mu_c(T)$, illustrates how the moment tends to vanish in a narrow temperature range (Figure 5). This is in agreement with the magnetization versus temperature, **M**(T), curve at 10 kOe, which displays a linear decrease up to about 10 K, followed by a faster decrease (Figure 5, inset). This behavior indicates that, due to

(20) Sato, M.; Takada, S.; Kohiki, S.; Babasaki, T.; Deguchi, H.; Oku, M.; Mitome, M. *Appl. Phys. Lett.* **2000**, *77*, 1194.

(21) Dorman, J. L.; Fiorani, D.; Tronc, E. *Adv. Ind. Chem. Phys.* **1997**, *98*, 283.
(22) Margeat, O.; Amiens, C.; Chaudret, B.; Lecante, P.; Benfield, R. E. *Chem. Mater.* **2005**, *17*, 107.
(23) Gambardella, P.; et al. *Science* **2003**, *300*, 1130.
(24) Linderoth, S.; Balcells, L.; Labarta, A.; Tejada, J.; Hendriksen, P. V.; Sethi, S. A. *J. Magn. Magn. Mater.* **1993**, *124*, 268.
(25) Batlle, X.; Labarta, A. *J. Phys. D: Appl. Phys.* **2002**, *35*, R15.

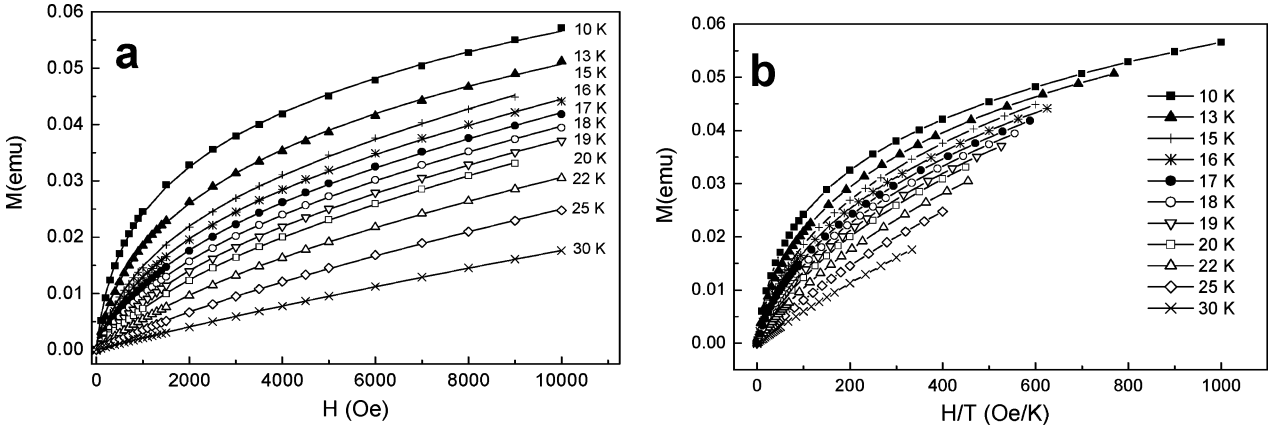

Figure 4. Magnetization loops versus T in the BetaCo samples: (a) magnetizations at different T values, (b) magnetization vs $\mathbf{H}/T$ corresponding to the curves shown in (a). The lines that link the experimental points correspond to the Langevin fit.

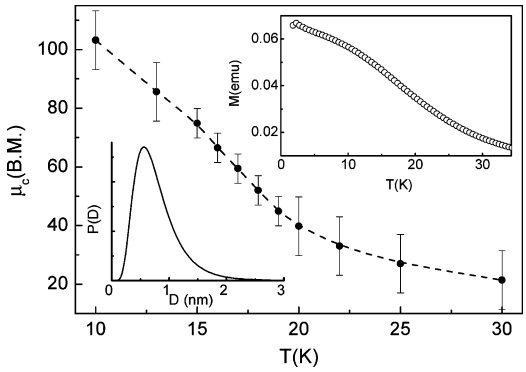

Figure 5. Magnetic moment per particle as a function of T in the BetaCo sample. Top inset: magnetization versus T at a 10 kOe field. Bottom inset: normalized size distribution for the BetaCo sample calculated from the fittings.

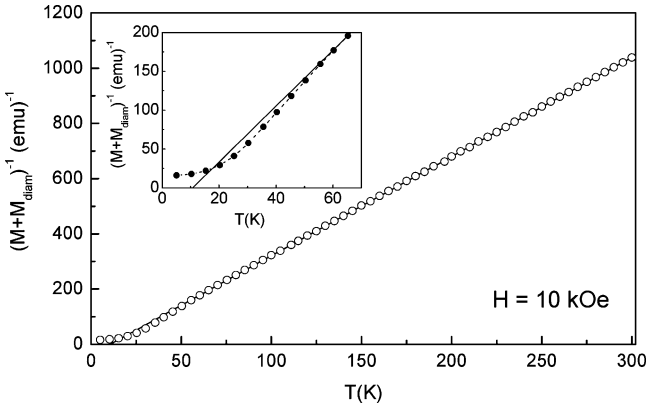

Figure 6. Departure from the Curie law in the BetaCo sample: inverse of the magnetization at 10 kOe. Inset: detail of the same curve at temperatures up to 65 K. The linear regime corresponds to a paramagnetic phase. A diamagnetic contribution independent of T coming from the matrix and the sample holder has been subtracted.

the reduced size of the clusters, the number of spins at the cluster surface dominates the $\mathbf{M}(T)$ behavior at low temperature (which is expected to be quasi linear),[25] while a faster demagnetization occurs at temperatures approaching T_c, as shown by Monte Carlo simulation.[26]

The nature of the magnetic coupling between cobalt atoms (ferromagnetic, antiferromagnetic, or ferrimagnetic) can be inferred from the $1/\mathbf{M}(T)$ curve (Figure 6), which follows a pure paramagnetic behavior between 50 and 300 K. The downward departure from the paramagnetic behavior observed below 50 K is evidence of the formation of magnetic moments in metallic cobalt, once the paramagnetic−ferromagnetic ordering is reached.[21] The extrapolated temperature from the linear regime at $1/\mathbf{M} = 0$ gives a value of 10 ± 2 K. This positive value also indicates ferromagnetic coupling between cobalt atoms, which is attributed to metallic bonding, since known cobalt oxides are antiferromagnetic and hydroxides are, as cobalt−silicon species, nonmagnetic (diamagnetic). The formation of Co^0 species from the original Co^{2+} in the framework can be easily explained by the reducing gases (CO and H_2) formed from the organic template during the calcination process.[12] The absence of a shift in the hysteresis loop after FC is further evidence of the absence of cobalt oxides.[8] Measurements of the sample before calcination show the diamagnetic contribution of the cobalt silicate matrix.

From the best fitting of the magnetization curves at all measured T values, we can extract a log-normal size distribution with a cobalt cluster average diameter of 0.8 nm (Figure 5, inset). The average volume of this distribution is 550 Å^3, corresponding to about 50 atoms of cobalt and a metallic cobalt content in the sample of 0.25 wt %. This is consistent with the average size and density of the clusters observed by TEM. In addition, this size distribution of the cobalt particles matches the size distribution of zeolite voids, indicating that the cobalt clusters grew inside the zeolite pores. From the obtained values and the extrapolation of μ_c at $T = 0$, an estimation of the magnetic moment per cobalt atom is extracted and a value of 2.2 μ_B calculated, which is similar to previously reported values for the same number of atoms.[2,3]

Longer heat treatments induce further segregation of atoms from the matrix, growth of the existing clusters, and a modification of the magnetic properties as would be expected. Thus, in the ZFC curve (Figure 7), a broader peak centered at lower T is observed together with a separation of the ZFC−FC curves (irreversibility) starting at 50 K, arising from both larger particles in the size distribution as a result of diffusive growth and smaller clusters coming from a matrix where cobalt is more diluted than in the first thermal treatment. This growth of the particles is seen by TEM where cobalt nanoparticles are now clearly observed (Supporting Information (S2)). The longer heat treatments also result in the presence of Co−CoO mixed crystals displaying exchange coupling and exchange bias.[8,27] This is clearly observed in an increased coercivity, an increase in the

(26) Iglesias, O.; Labarta, A. *Phys. Rev. B* **2001**, *63*, 184416.

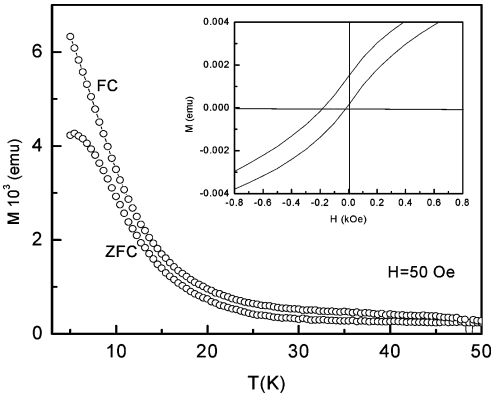

Figure 7. ZFC−FC magnetization for the annealed sample. The sample was heated for 5 h at 750 °C (including a 3°/min heating ramp) under N_2 and 6 h at 750 °C open to air. Inset: detail of the hysteresis loops at 5 K after 1 T field cooling, where the curve is shifted in **H** in the direction opposite that of the applied field (10 kOe) during cooling.

irreversibility field (where the hysteresis loop closes), and, mainly, a shift of the hysteresis loop, after field cooling, in the direction opposite that of the applied field (10 kOe) during cooling (Figure 7, inset). The same experiment in the calcined samples did not show any of these features. At intermediate longer heat treatments, intermediate effects were observed (Supporting Information (S3)).

As a control experiment, another zeolite, ZSM-5Co, with a maximum internal void diameter of ∼0.8−1.0 nm at the crossing of channels was synthesized with 2.5 wt % cobalt. The structural and magnetic properties are essentially the same, and T_B is 8.9 and 9.6 K in BetaCo and ZSM5Co, respectively (Supporting Information (S4)), indicating that cobalt clusters are similar. This is remarkable since one could expect, for the same heat treatment, the BetaCo clusters to be larger because the amount of available cobalt is larger (5 wt %). This fact indicates that the dimensions of the internal void in the pores and cavities is dominant and that, at moderate heat treatments, the final cluster size distribution is strongly conditioned by the 3D spatial distribution of those pores and cavities. This confinement also plays a crucial role in stabilizing the particles.[28] Therefore, when clusters grow larger with extended heat treatments and escape from confinement, an antiferromagnetic phase corresponding to cobalt oxide is detected (Supporting Information (S5)). Metal passivation by confinement should be related to both the special electromagnetic environment inside the zeolite cavities[29] and the lower density of cobalt oxides with respect to cobalt. Indeed, when the metal cobalt cluster is occupying the full cavity, there is no room left to oxidize the cobalt for oxygen. Other distributions of very small metal fractions inside zeolite pores leading to special magnetic behavior have been described in ref 30.

In conclusion, we have prepared highly stable subnanometric cobalt clusters whose metallic character is preserved after open-air heat treatments and for which the magnetic signal is constant after months at room conditions. These metallic cobalt clusters exhibit an extremely low ferromagnetic ordering temperature. This extremely low T_c leads to a mixed SPM and ferromagnetic−paramagnetic transition behavior and therefore to the narrowest vanishing of the magnetic moment observed in particles of 3d ferromagnetic materials.

Acknowledgment. We are grateful to Dr. Josep Nogues for helpful discussion and critical reading of the manuscript, to Dr. Jordi Arbiols for high-resolution TEM, and to Dr. Patricia Concepcion for XPS analysis. This work was supported by the Generalitat de Catalunya (Grups Consolidats 2001 SGR 00066) and Ministerio de Educación y Ciencia (Grants MAT2003-01124 and MAT2003-07945-C02-01).

Supporting Information Available: XRD spectra of BetaCo and ZSM-5-Co as-synthesized and calcined without peaks of magadiite and any metallic cobalt compound, UV−vis spectra of BetaCo as-synthesized and calcined showing the presence of tetrahedrally coordinated Co^{2+}, low-resolution TEM (the absence of visible metallic particles and the morphology of the zeolite grains can be observed at magnifications between 50000 and 100000), fitting of the magnetization loops (the Langevin fit of the magnetization loops allows the magnetic moment per particle and simultaneously the value of the magnetization per volume unit and the particle size distribution to be obtained), longer heat treatments (the magnetization measurements and microscopy of the samples annealed for longer times, and at higher temperatures, show the growth, migration, and oxidation of the cobalt particles), BetaCo vs ZSM5Co after calcination (the ZFC magnetization of both samples shows a small shift of the mean blocking temperature T_B (8.9−9.6 K)), and complete list of author citations with more than 10 authors. This material is available free of charge via the Internet at http://pubs.acs.org.

JA053746B

(27) Verelst, M.; Ely, T. O.; Amiens, C.; Snoeck, E.; Lecante, P.; Mosset, A.; Respaud, M.; Broto, J. M.; Chaudret, B. *Chem. Mater.* **1999**, *11*, 2702.
(28) Kim, S.; Son, S. U.; Lee, S. I.; Hyeon, T.; Chung, Y. K. *J. Am. Chem. Soc.* **2000**, *122*, 1550.
(29) Zicovich-Wilson, C. M.; Corma, A.; Viruela, P. *J. Phys. Chem.* **1994**, *98*, 10863.
(30) Nozue, Y.; Kodaira, T.; Ohwashi, S.; Goto, T.; Terasaki, O. *Phys. Rev. B* **1993**, *48*, 12253.